Tomographic analysis of self-potential data in a seismic area of Southern Italy

Vincenzo Lapenna ([1]), **Domenico Patella** ([2]) **and Sabatino Piscitelli** ([1])
([1]) *Istituto di Metodologie Avanzate di Analisi Ambientale, CNR, Tito (PZ), Italy*
([2]) *Dipartimento di Scienze Fisiche, Università «Federico II», Napoli, Italy*

Abstract
The time and space anomalous behaviour of the Self-Potential (SP) field recorded in a seismic area of Southern Apennines, Italy, is discussed. The SP data were collected in the period June 1992-November 1994 along a profile located north of the town of Potenza in the Basilicata region, Italy. The profile is perpendicular to an active fault system, where a W-E directed strike-slip structure has been identified from recent earthquakes. The SP data are modelled using a new tomographic method based on the search for similarities between the observed SP sequence and the surface signature of the electric field due to a scanning point source with unitary positive charge. The point scanner is ideally moved in a vertical cross-section through the profile and a regular 2D matrix of charge occurrence probability values is thus obtained. These values are used to image the state of electric polarization in the subsoil, compatible with the observed SP surface pattern. A selection of 2D tomographies across the profile is then discussed in order to outline the SP source geometry and dynamics within the faulted structure. Finally, the time pattern of the SP polarization state is compared with the local seismicity in the frame of the rock dilatancy-fluid diffusion theory. This comparison allows us to exclude a direct relationship of the SP time behaviour with the seismic sequences which occurred in the area during the SP monitoring period.

Key words *self-potential – tomographic technique – fault system – Southern Apennines*

1. Introduction

The deterministic approach to the earthquake prediction problem has long attracted many scientists all over the world. Experimental observations have been carried out in many active seismic areas in order to detect anomalous changes in geophysical parameters before and during earthquakes. In particular, great attention has been paid to the electric parameters. Among the most debated contributions we quote the unusual geoelectric anomaly detected in China before the 1975 Haicheng earthquake (Chu *et al.*, 1996), the controversial earth's current recording network acting in Greece to predict local earthquakes (Varotsos *et al.*, 1993) and the intensive studies done in U.S.A. to detect resistivity changes during the Parkfield experiment (Park, 1997).

However, in all the experiments showing the occurrence of electric anomalous signals in seismic areas the correlation with the local seismicity is barely documented. The main weak point is that the observations are generally so sparse in time and space that only rarely can robust statistic tests be applied to evaluate the reliability of the anomalous signals as precursory events (Geller, 1997; Geller *et al.*, 1997; Cuomo *et al.*, 1998).

Mailing address: Dr. Vincenzo Lapenna, Istituto di Metodologie Avanzata di Analisi Ambientale, CNR, C.da S. Loja, Zona Industriale, 85050 Tito Scalo (PZ), Italy; e-mail: lapenna@unibas.it

The model that is most commonly used to explain the occurrence of electric signals in seismic areas is the dilatancy-diffusion-polarization theory (Nur, 1972; Mizutani *et al.*, 1976; Morgan *et al.*, 1989; Scholtz, 1990; Patella *et al.*, 1997). According to this model, if a stressed rock in a focal region is saturated with ionized water the formation of cracks due to rock dilatancy generates a pressure gradient forcing the liquid to invade the new voids. The fluid flow lasts until pressure balances across the newly created system of interconnected pores. In stable conditions before dilatancy, a double layer normally exists between free cations in the saturating liquid and anions adsorbed to the pore walls. When the liquid is forced to flow through the porous medium, the water molecules carry along with them free positive ions in the diffusion part of the pores. The displacement of these cations with respect to the firmly attached anions breaks the double layer and generates the so called streaming potential. As suggested by Mizutani *et al.* (1976), the creation of the double layer and the streaming potential accompanying the fluid motion towards the dilatant zone can be responsible for the anomalous voltages that are measured on the ground surface preceding an earthquake.

Significant results regarding the observation of electrokinetic effects were obtained in volcanic and geothermal areas (Corwin and Hoover, 1979; Nishida and Tomiya, 1987; Zlotnicki *et al.*, 1994; Di Maio *et al.*, 1998; Jonsthon, 1997; Revil and Pezard, 1998) and from laboratory experiments (Jouniaux and Pozzi, 1995).

A Self-Potential (SP) anomalous pattern is the free surface evidence of a more or less unstable state of electric charge polarization in the subsoil. Thus, the SP inverse problem actually consists in delineating the location and geometry of any electric sources distribution underground. Recently, Patella (1997) proposed a new method of SP data interpretation based on the cross-correlation between the field generated by an elementary SP source located anywhere in the subsoil and the observed SP surface field. A normalized cross-correlation function was introduced to estimate the occurrence probability of electrical charges at the nodes of a regular grid within the surveyed volume. Finally, all the charge occurrence probability values are contoured in order to draw tomographic images of the subsoil showing the zones where the probability of detecting charge accumulations is higher.

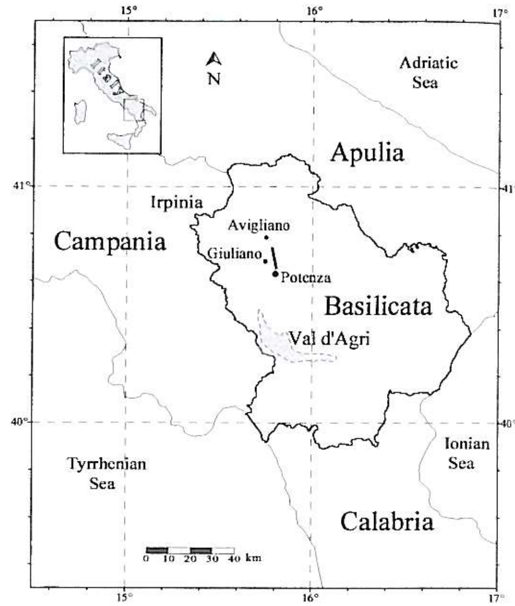

Fig. 1. Location of the monitored profile on the Southern Apennine chain (Italy).

In this paper we show the results of the application of this tomographic approach to a set of SP data recorded periodically from June 1992 to November 1994 along a profile crossing an active fault system of the Southern Apennines, located north of the town of Potenza, Basilicata region, Italy (see fig. 1). The repeated surveying combined with a powerful imaging technique of the local SP field can give a dynamical description of the electrical charges motion near the focal area. This approach can be useful to study the relationship between tectonic processes and electric anomalous signals.

2. Geological and seismological outline of the survey area

The survey area is located in the Campanian-Lucan Apennine range (Southern Italy). It is limited to the north by the village of Avigliano and to the south by the periphery of the town of Potenza (fig. 2).

The structural setting of the survey area consists of a pile of thrust sheets resulting from a sequence of tectonic events associated with the collision between the African and European plates along the southern margin of the Tethys ocean (Pantosti and Valensise, 1990).

During the Mesozoic and Early Cenozoic different large and thick carbonate platforms developed along this margin. These platforms

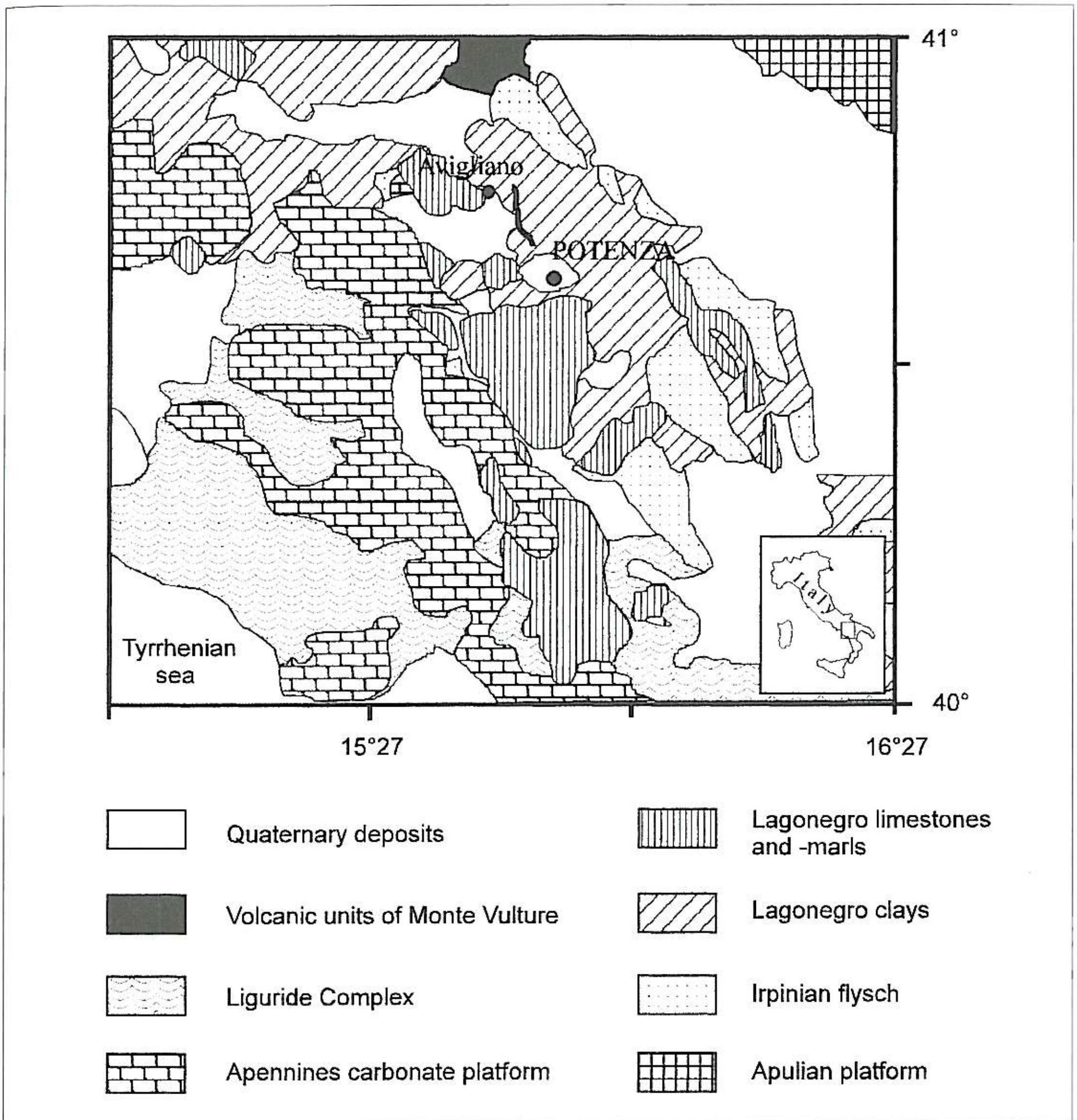

Fig. 2. Geological map of the investigated area.

were surrounded by deeper terrigenous basins, the innermost of which are of oceanic type. Starting from the Middle Miocene up to the Upper Pliocene, several compressional tectonic phases caused progressive thrusting and piling of different tectonic units, corresponding with different paleogeographic domains, towards stable external domains of the Apulian-Adriatic foreland (Patacca *et al.*, 1988). The deformation front direction was initially NW-SE, then migrated toward NE. During the Quaternary, the Southern Apennines were affected by an important extensional tectonic phase with a NE-SW extensional trend that caused further fragmentation of the chain into several isolated blocks.

Several distinct stratigraphic and tectonic units characterize the survey area, but the name, age and correct position of each unit is still a matter of debate (D'Argenio *et al.*, 1973; Pescatore *et al.*, 1988). In the map in fig. 2 we observe that the main outcropping terrains are ascribable to flyschoid units normally composed of an alternance of limestones, calcarenites, marls, clays and shales, dating from the Jurassic to Lower Miocene (Tertulliani *et al.*, 1992). Structurally, the survey area is dominated by sheet thrusting hardly deformed towards NE and NNE and widespread extensional fracturing.

We carried out a geoelectric prospect in the survey area in order to better define the local geological structures. In particular, we applied the dipolar pseudosection method along the same profile used for the SP survey (see fig. 3). Figure 4 shows the pseudosection imaging of the

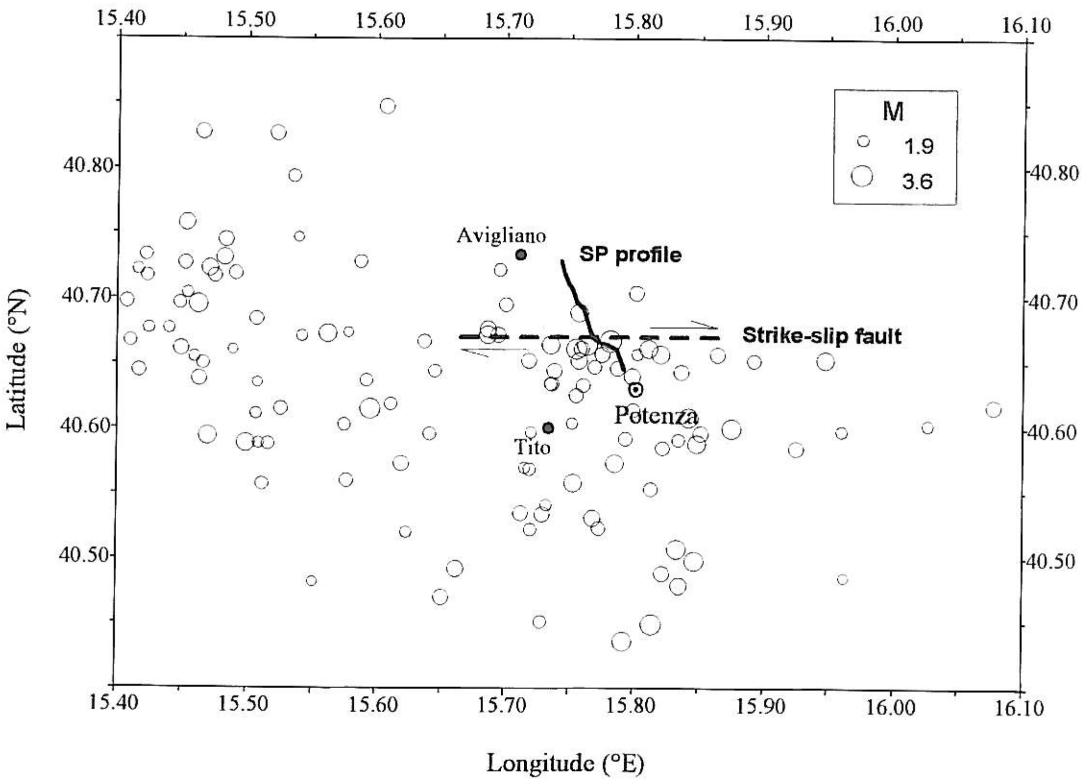

Fig. 3. Spatial seismicity pattern observed during the period June 1992-November 1994 in the investigated area. The size of the circles is related to the magnitude ($M = 1.9 \div 3.6$). The SP profile is quite perpendicular to the strike-slip fault inferred from seismology.

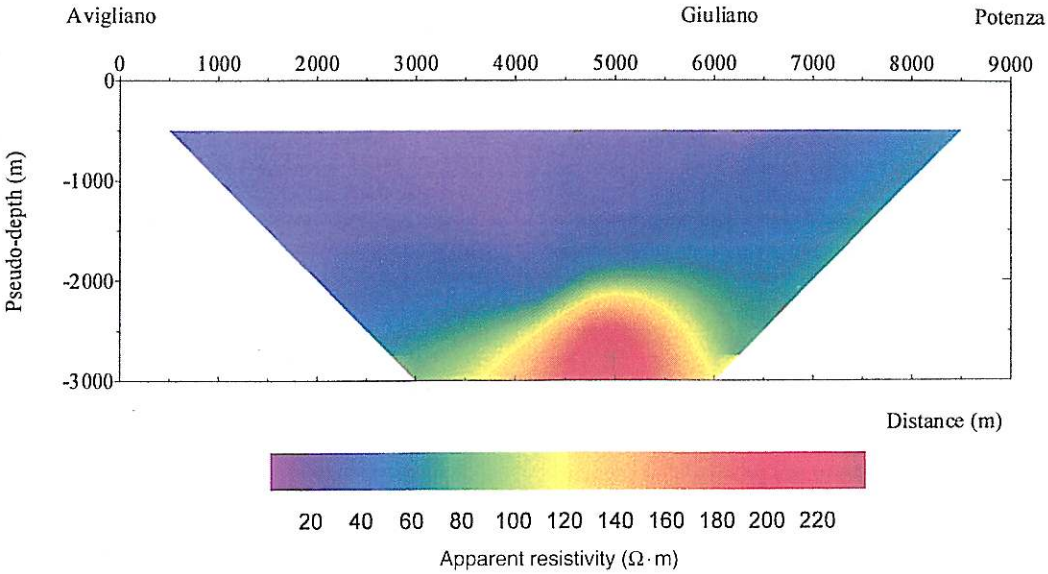

Fig. 4. Dipole-dipole resistivity pseudosection along the same profile selected for the SP measurements.

dipole survey. The apparent resistivity ρ_a values regularly increase with depth varying over a very small range from less than 20 $\Omega\cdot$m to more than 200 $\Omega\cdot$m. Globally, these ρ_a values reflect a low degree of lateral and vertical inhomogeneity in the section. In particular, values with $\rho_a \leq 100\ \Omega\cdot$m, appearing down to a mean pseudodepth of 2000 m, may be ascribed to conductive materials such as clays and/or shales. In the central part, beyond 2000 m of pseudodepth, a horst-like structure with $\rho_a \geq 100\ \Omega\cdot$m may be associated with resistive materials, like limestones and/or calcarenites.

Historical and instrumental seismic data extracted from the catalogues of the National Institute of Geophysics (ING) and the Vesuvian Observatory lead us to consider the Lucan Apennines one of the most active seismogenetic areas in Southern Italy. In particular, the area around Potenza shows a seismicity characterized by rather frequent seismic sequences with intensities not larger than VII (MCS). The investigated area has also been hit by destructive events in surrounding regions as in Irpinia (1694, 1930, 1980) and Val d'Agri (1857) (Tertulliani *et al.*, 1992).

The seismological analysis of the last remarkable events that affected the area around Potenza on May 5, 1990, $M_D = 5.0$, and May 26, 1991, $M_D = 4.5$, where M_D is the duration magnitude, demonstrates that these earthquakes were generated by a strike-slip fault in an E-W direction, *i.e.* nearly perpendicular to the Apennine chain. This fault lies north of Potenza and is located in such a way as to cross to north and south the two great seismogenetic faults that caused the 1980 Irpinia and 1857 Val d'Agri earthquakes, respectively. The frequent strong events in the survey area can thus be explained by the fact that at least three independent seismogenetic structures can be affected (Boschi *et al.*, 1994; Lapenna *et al.*, 2000). The aftershocks of the above mentioned 1990 and 1991 events also show a distinct E-W trend and appear to define a roughly vertical plane. They are concentrated between 15 and 25 km in depth and outline a 200 km^2 fault area extending approximately 20 km in length and 10 km in depth. For these events a source depth between 9 and 15 km has been estimated (Ekström, 1994).

In particular, during the monitoring period the national seismometric network of the National Institute of Geophysics detected 117 earthquakes with magnitude varying in the range 1.9-3.6. The spatial distribution of these events shows a weak cluster effect close to the fault system (fig. 3).

3. Data presentation and preliminary analysis

During the period June 1992-November 1994, 18 SP surveys were carried out to measure the time changes of the SP field along a profile located north of Potenza (fig. 3). The length of the profile is 9400 m.

The SP data were collected as potential drops across a passive dipole 200 m in length, continuously displaced along the profile. The measuring system consisted of two non-polarizable electrodes put into the ground and connected with insulated cables to a data-logger with high sensitivity (1μV), high input-impedance ($R > 1\mathrm{M}\Omega$) and a low-pass filter circuit to remove electromagnetic cultural noise. The measuring system was linked to a PC and a software routine was applied to check the acquisition procedure and to remove outliers. In each station the voltage signal was recorded for 10 min with a sampling interval Δt = 1 s. Then, the mean value of the recorded data was estimated and stored.

We assume that the electrical field on earth surface is quite constant during the SP measurements, the period of field survey being shorter than 4 h. This is a reasonable constraint when there are no thunderstorms and/or magnetic changes close to the investigated area. Thus, the SP value $V(x)$ in any point of the profile was easily obtained using the formula

$$V(i\Delta x) = \sum_{j=1}^{i} \Delta V_j + V(0), \quad \text{for } i = 1, \ldots N \tag{3.1}$$

where Δx is the dipole length, ΔV_j are the meas-

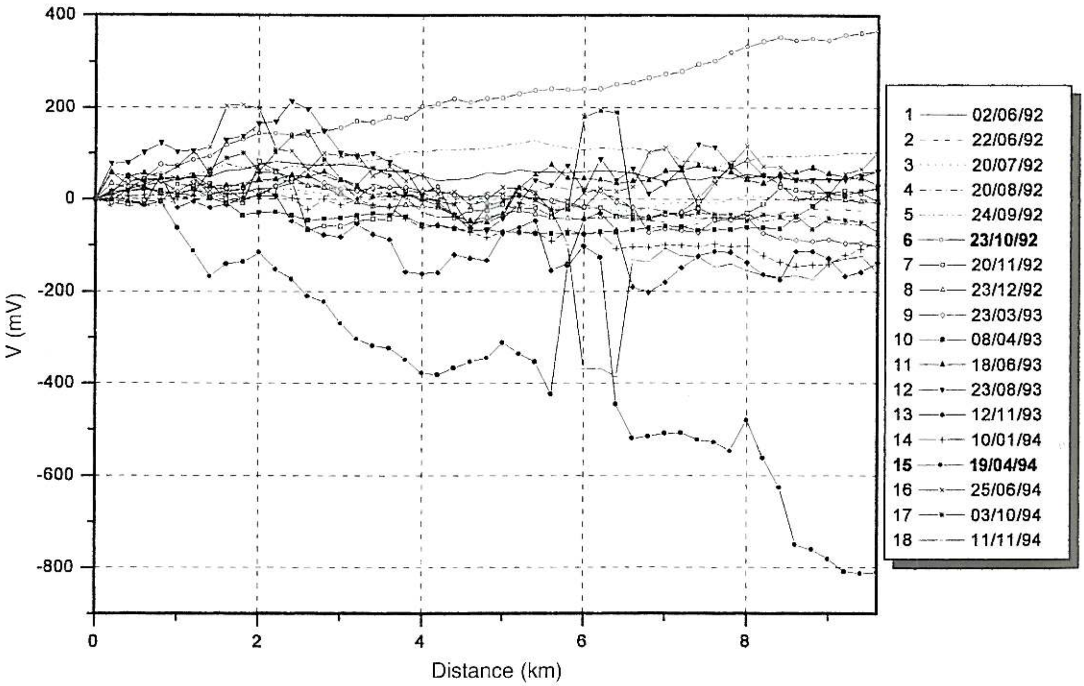

Fig. 5. Diagrams of 18 SP profiles measured in the investigated area.

ured voltage differences, $V(0)$ is the SP value at reference point (the origin of the profile) arbitrarily assumed equal to zero and N is the total number of measurements.

Figure 5 shows the diagrams of the 18 experimental SP surveys. We do not report the instrumental errors on the graph because they are negligible ($< 10 \mu V$). The main errors associated with our estimates are mainly due to topographic irregularities, near-surface geological discontinuities and high frequency fluctuations of electrical field on earth surface. This kind of errors produces sharp fluctuations in the SP profiles and, as a consequence, high frequency anomalies in the shallow part of the tomographic images.

The two profiles no. 6 and no. 15 display a pattern which visibly departs from that of all the

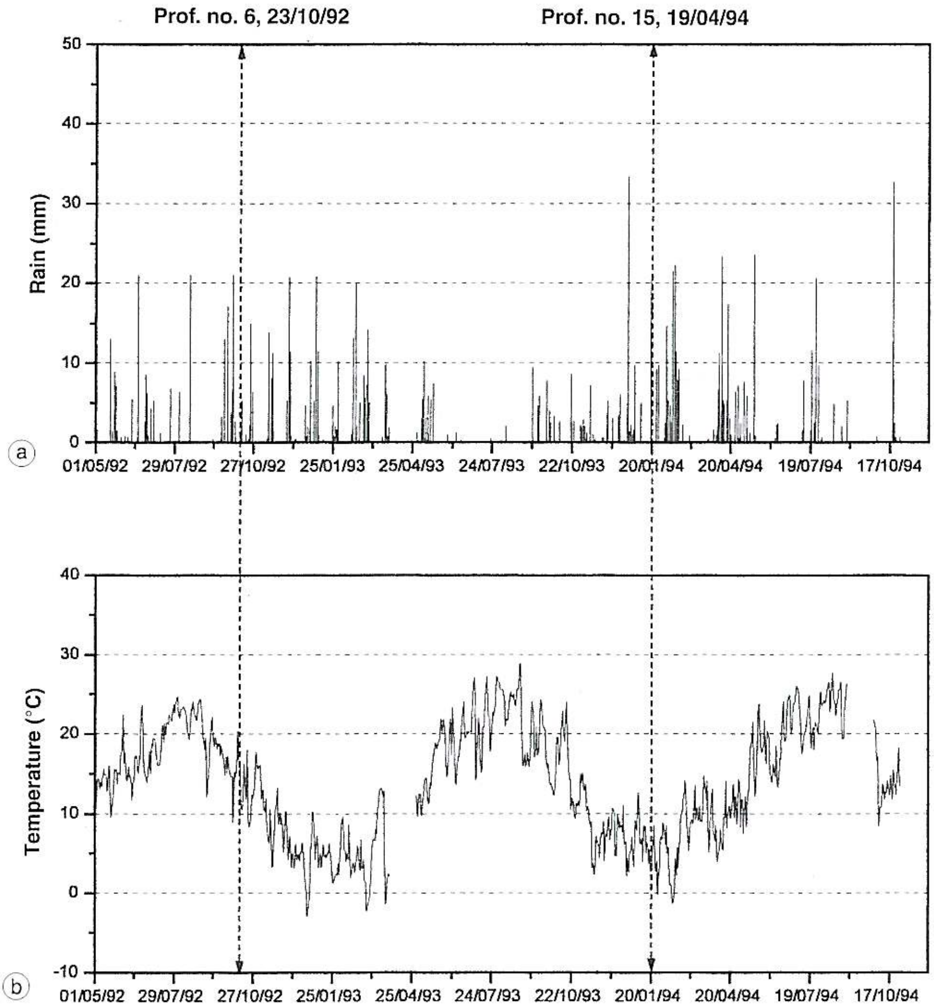

Fig. 6a,b. Climatological data measured at Potenza during the SP monitoring period. The daily rainfall is reported in fig. 6a and the daily mean temperatures in fig. 6b. The data are extracted from the Bulletin of the *Servizio Idrografico*.

other profiles. Indeed, profile no. 6 is characterised by a smooth constant increase in the SP signal, whereas profile no. 15 shows a steep negative SP gradient. The comparison of the SP survey data with the climatological records in the area allowed us to exclude a correlation of the SP profiles no. 6 and no. 15 with extreme meteoclimatic events (fig. 6a,b). Hence we considered these two profiles anomalous and deserving a proper explanation. A tomographic technique was then adopted to try to reconstruct the charge polarisation state in the subsoil, responsible of the observed anomalous SP patterns.

4. Short description of the tomographic technique

We briefly describe the mathematical background of the 2D probability tomography technique recently proposed by Patella (1997). We adopted this technique to interpret the SP surveys along the profile located north of Potenza.

The probability tomography is based on the decomposition of the SP field into a sum of elementary contributions due to a discretised distribution of charge accumulation centres. The inversion problem consists in recovering the most probable discretised charge distribution underground, responsible of the measured SP field. The 2D tomography is based on a cross-correlation algorithm between a theoretical scanner function and the observed SP electric field. In the 2D case a Charge Occurrence Probability (COP) function $\eta(x_q, h_q)$ is defined as (Patella, 1997)

$$\eta(x_q, h_q) = C h_q^{3/2} \int_{-\infty}^{+\infty} E_x(x) \Im_x(x - x_q, h_q) dx, \tag{4.1}$$

$$\text{for } h_q > 0$$

where E_x is the electric field component along the x-axis, estimated from the SP drops measured along the profile, (x_q, h_q) is the pair of coordinates of a generic point in the vertical cross-section through the profile, C is a normalisation factor given by

$$C = \frac{2 \cdot 2^{1/2}}{\left[\eta \int_{-\infty}^{+\infty} E_x^2(x) dx \right]^{1/2}}. \tag{4.2}$$

and $\Im_x(x - x_q, h_q)$ is the scanner function given as

$$\Im_x(x - x_q, h_q) = \frac{(x - x_q)}{[(x - x_q)^2 + h_q^2]^{3/2}}. \tag{4.3}$$

The application of Schwarz's inequality for the derivation of $\eta(x_q, h_q)$ implies that the COP function is constrained to vary inside the interval

$$-1 \leq \eta(x_q, h_q) \leq +1. \tag{4.4}$$

In a statistical sense, the COP function $\eta(x_q, h_q)$ represents the probability of finding in a point (x_q, h_q) of the cross-section through the profile a positive ($\eta > 0$) or negative ($\eta < 0$) electric charge accumulation, which is responsible for the whole field observed on the surface. Obviously, for practical application a discretised version of (4.1) is useful. This can be found in Patella (1997).

The 2D tomographic approach is now explained using a synthetic example (fig. 7). We fixed two elementary charges (negative and positive) at the points $(-6, -5)$ and $(+6, -5)$ in the (x, h)-plane, respectively. Arbitrary units were used. Firstly, the electric field component $E_x(x)$ was computed, then formula (4.1) was applied and finally the $\eta(x_q, h_q)$ values were contoured in the (x, h) tomoplane. As expected, the maximum COP values, close to $+1$, were obtained in correspondence with the points where the positive charges were located.

5. Experimental results and discussion

We analyse the results obtained applying the new tomographic technique to the SP profiles measured close to the active fault located on the northern side of the town of Potenza. For brev-

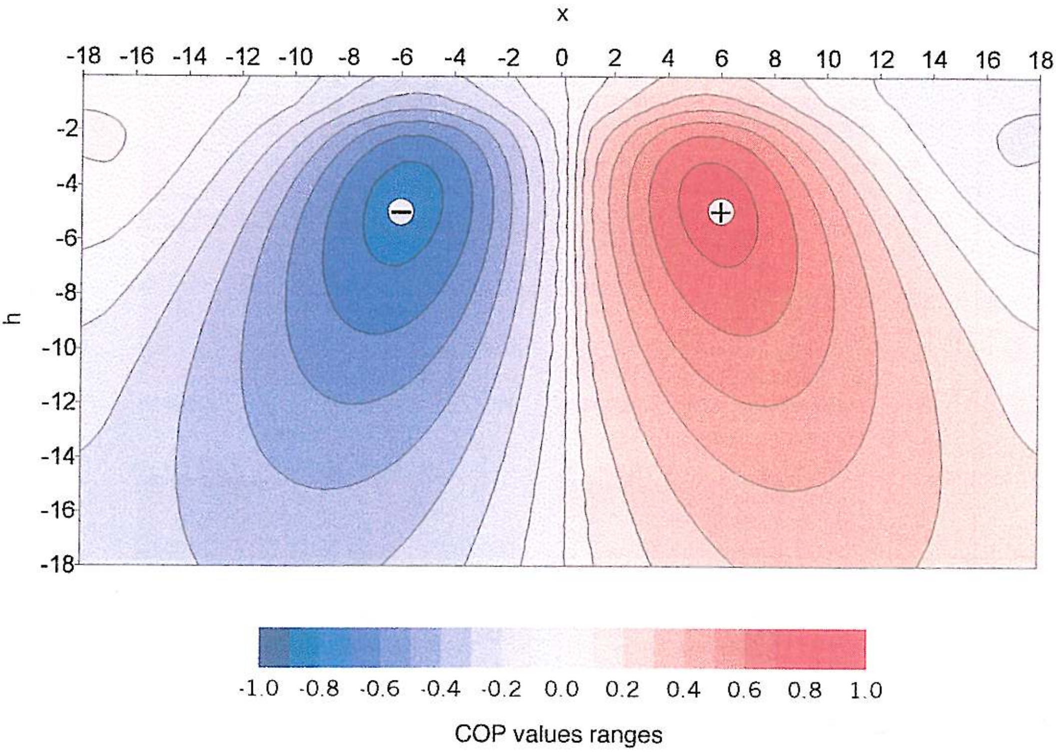

Fig. 7. The 2D probability tomography imaging relative to a simulation.

ity we only consider the tomographic images of 6 profiles out of the set of 18.

Figure 8 shows the 2D representation of the COP values for the 6 selected SP profiles. In each tomography the horizontal axis is the survey line and the vertical axis is the depth. The centre of the profile is indicated with 0 offset distance and the positive and negative distances are directed northward and southward, respectively. For computation we used a square grid with side of 200 m, equal to the field sampling interval.

Firstly, we observe in the shallowest part of all the tomoplanes a scattered sequence of charge accumulations ascribable to near-surface discontinuities. Electrokinetic effects induced by meteoric water percolation and evaporation can be invoked to explain these shallow features. Then, we observe a variable long wavelength dipolar field reflecting the presence of the fault system in the investigated area.

In particular, the first image, which refers to profile no. 1, suggests the presence of a negative charge concentration on the right-hand side of the profile and a positive charge distribution on the left with barycentres located at about 1 km in depth. The tomographic image associated with the anomalous profile no. 6 suggests, instead, a concentration of charges in the deepest part of the section. A dipolar field configuration is evident with the positive and negative nuclei localised on the right and left sides of the tomoplane, respectively, at a depth not less than 3-4 km. In all the following pictures, no remarkable deep polarisation seems worth commenting, except for a slightly perceptible tendency of the deep dipole to invert its polarity. Indeed, compared with the deep pattern appearing in profile no. 6, the images relative to profiles no. 15 and no. 18 show a weak regional field with reversed polarity, while

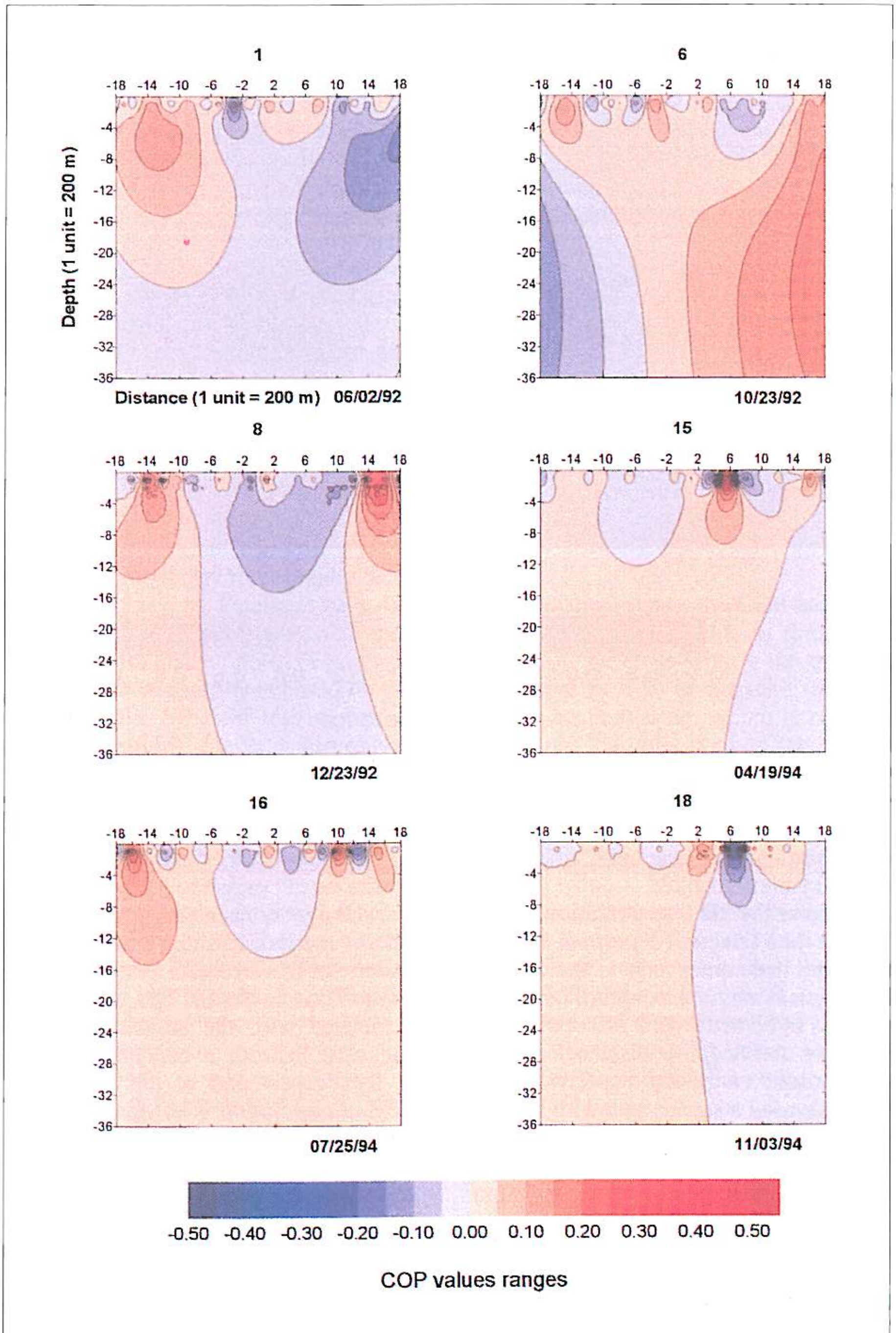

Fig. 8. The 2D probability tomography imaging of 6 selected SP profiles.

Table I. List of seismic events extracted from the catalogue of the ING after applying the Dobrovolsky algorithm. The SP profiles measured during the period June 1992-November 1994 are also indicated.

Profile no.	Latitude (°N)	Longitude (°E)	Depth (km)	M_d	Date	Distance (km)
	40.695	15.462	7.643	3.3	June 2, 1992	25.1
1					*June 2, 1992*	
	40.704	15.801	8.963	2.6	June 16, 1992	3.5
	40.664	15.735	7.513	3.0	June 18, 1992	4.5
2					*June 22, 1992*	
	40.634	15.735	9.516	2.3	July 12, 1992	7.6
3					*July 20, 1992*	
	40.634	15.736	5.000	2.5	August 4, 1992	7.6
4					*August 20, 1992*	
	40.661	15.759	7.364	2.6	September 16, 1992	4.3
5					*September 24, 1992*	
6					*October 23, 1992*	
7					*November 20, 1992*	
8					*December 23, 1992*	
	40.664	15.763	10.000	3.4	January 24, 1993	4.0
	40.652	15.757	10.000	2.9	March 20, 1993	5.3
9					*March 23, 1993*	
	40.661	15.755	5.000	3.5	April 5, 1993	4.4
10					*April 8, 1993*	
	40.507	15.833	10.000	3.2	May 25, 1993	22.3
	40.573	15.785	5.000	3.1	June 3, 1993	14.3
11					*June 18, 1993*	
	40.615	15.595	5.000	3.4	August 16, 1993	16.8
12					*August 23, 1993*	
	40.614	15.799	10.000	2.4	September 16, 1993	10.1
13					*November 12, 1993*	
	40.652	15.718	5.000	2.6	December 5, 1993	6.4
14					*January 10, 1994*	
	40.661	15.811	5.000	3.1	February 13, 1994	6.1
	40.722	15.695	10.000	2.3	March 17, 1994	6.0
15					*April 19, 1994*	
	40.643	15.836	9.202	2.7	April 21, 1994	9.0
	40.558	15.753	5.000	3.1	April 23, 1994	15.8
	40.695	15.700	21.055	2.4	May 27, 1994	5.1
	40.676	15.686	5.000	2.8	June 14, 1994	6.8
	40.625	15.755	5.000	2.5	June 14, 1994	8.3
	40.657	15.864	9.315	2.6	June 23, 1994	10.0
16					*June 25, 1994*	
	40.672	15.694	5.000	2.6	August 6, 1994	6.4
	40.673	15.562	5.000	3.1	August 12, 1994	16.9
	40.647	15.769	10.000	2.5	September 6, 1994	5.9
17					*October 3, 1994*	
	40.672	15.686	9.311	3.1	November 1, 1994	7.0
18					*November 11, 1994*	
	40.449	15.814	5.000	3.5	November 12, 1994	28.3

profiles no. 8 and no. 16 show intermediate patterns.

The geological setting of the investigated area and the presence of fluids underground suggested us to consider the temporal variations of the COP function as a consequence of electric charge redistribution. As previously mentioned, a known physical mechanism is the streaming potential effect triggered by crustal strains. In the several seismic cycles the focal region is submitted to time and space variations of the stress field. During an inter-seismic period the strain increase produces a dilatant region all around the faulted area. The decrease of hydraulic pressure due to dilatancy triggers a large-scale fluid flow into the dilated region from surrounding saturated zones. Thus, the water flow produces a net separation of charges generating an anomalous electric potential and a positive anomaly of the SP field over the dilatant zone. At the time of the earthquake cracks close and water is expelled. At this stage we expect a depolarisation process re-establishing a neutral electrical configuration.

On the basis of such a physical process we investigated a possible correlation between the charge motion detected in the survey area and the earthquakes which occurred during the monitoring activity. A preliminary problem to be solved was to select from the seismic catalogue only the events that, in principle, can produce strain effects in the investigated area. For this purpose we used Dobrovolsky's criterion (Dobrovolsky, 1992) based on the empirical relationship

$$r = 10^{0.43M} \tag{5.1}$$

where M is the magnitude and r is the radius of the area in which the effects of the earthquake are detectable.

Table I lists all the seismic events with r smaller than the epicentral distance R, selected from the catalogue of ING.

A slowly increasing seismic activity occurs after the execution of SP profile no. 15, whose tomography, however, does not disclose any particular charge dislocation. On the contrary, there is no seismic sequence before and after the execution of SP profile no. 6, whose tomography, however, shows an evident deep charge polarisation.

Accounting for this preliminary analysis, our present opinion is that the change in the charge distribution in the subsoil along the profile located to the north of Potenza seems not directly related to the local earthquake activity. It may be connected, instead, to fluid movements triggered by slow stress variations. Obviously this is only a very preliminary tentative correlation. We do not yet have a significant statistical basis to obtain a true quantitative evaluation of the correlation existing between charge movements and local seismic activity.

6. Conclusions

A first application of a new tomographic methodology has been applied to detect the underground charge movements in a seismic area of the Southern Apennine chain. The first results allow us to consider this approach well suited to analyse the space and time dynamics of parameters of electrical nature in seismic areas. Only from the observed SP data (map and/or profiles) is it possible to have a statistical evaluation of the probability to find positive/negative electrical charge concentrations in the subsoil. Combining this technique with a monitoring strategy based on a very dense distribution of remote measuring stations around well selected focal areas, in the near future we shall probably be able to obtain more reliable results about the possible generation of electrical signals during an earthquake cycle. In our opinion this new methodological approach can be considered a promising tool to investigate spatial and time dynamical patterns of the electrical field in seismic areas.

REFERENCES

BOSCHI, E., D. PANTOSTI and G. VALENSISE (1994): L'identificazione geologica delle faglie sismogenetiche, *Le Scienze*, **310**, 36-46.

CHU, J.J., G. XIETAI, D. JINGAN, C. MARONE, M.W. SPIEGELMAN, L. SEEBER and J.G. ARMBRUSTER (1996): Geoelectric signals in China and the earthquake ge-neration process, *J. Geophys. Res.*, **101**, 13869-13882.

CORWIN, R.F. and D.B. HOOVER (1979): The self-potential method in geothermal exploration, *Geophysics*, **44**, 226-245.

CUOMO, V., V. LAPENNA, M. MACCHIATO, C. SERIO and L. TELESCA (1998): Linear and non linear dynamics in electrical precursory times series. implications with earthquake prediction, *Tectonophysics*, **287**, 279-298.

D'ARGENIO, B., T. PESCATORE and P. SCANDONE (1973): Schema geologico dell'Appennino Meridionale (Campania e Lucania), in *Atti del Convegno «Moderne Vedute sulla Geologia dell'Appennino», Rend. Accad. Naz. Lincei*, **183**, 49-72.

DI MAIO, R., P. MAURIELLO, D. PATELLA, Z. PETRILLO, S. PISCITELLI and A. SINISCALCHI (1998): Electric and electromagnetic outline of the Mount Somma-Vesuvius structural setting, *J. Volcanol. Geotherm. Res.*, **82**, 219-238.

DOBROVOLSKY, I.P. (1992): Analysis of preparation of a strong tectonic earthquake, *Phys. Solid Earth*, **28**, 481-492.

EKSTRÖM, G. (1994): Teleseismic analysis of the 1990 and 1991 earthquakes near Potenza, *Ann. Geofis.*, **37** (6), 1591-1599.

GELLER, R.J. (1997): Earthquake prediction: a critical review, *Geophys. J. Int.*, **131**, 425-450.

GELLER, R.J., D.D. JACKSON, Y.Y. KAGAN and F. MULARGIA (1997): Earthquake cannot be predicted, *Science*, **275**, 16/6.

JONSTHON, M.J.S. (1997): Review of electric and magnetic fields accompanying seismic and volcanic activity, *Surv. Geophys.*, **18**, 441-475.

JOUNIAUX, L. and J.P. POZZI (1995): Streaming potential and permeability of saturated sandstones under triaxial stress: consequences for electrotelluric anomalies prior to earthquakes, *J. Geophys. Res.*, **100**, 10197-10209.

LAPENNA, V., M. MACCHIATO, S. PISCITELLI and L. TELESCA (2000): Scale invariance properties in seismicity of Southern Apennine chain (Italy), *Pure Appl. Geophys.*, **157** (in press).

MIZUTANI, H., T. ISHIDO, Y.YOKOKURA and S. OHNICHI (1976): Electrokinetic phenomena associated with earthquake, *Geophys. Res. Lett.*, **3**, 365-369.

MORGAN, F.D., E.R. WILLIAMS and T.R. MADDEN (1989): Streaming potential properties of westerly granite with applications, *J. Geophys. Res.*, **94**, 12449-12461.

NISHIDA, Y. and H. TOMIYA (1987): Self-potential studies in volcanic areas (1) - Usu volcano, *J. Fac. Sci., Hokkaido Univ., Ser. VII*, **8**, 173-190.

NUR, A. (1972): Dilatancy pore fluids, and premonitory variations of tp/ts travel time, *Bull. Seismol. Soc. Am.*, **62**, 1217-1222.

PANTOSTI, D. and G. VALENSISE (1990): Faulting mechanism and complexity of the November 23, 1980, Campania-Lucania earthquake, inferred from surface observations, *J. Geophys. Res.*, **95**, 15319-15341.

PARK, S.K. (1997): Monitoring resistivity changes in Parkfield, California 1988-1995, *J. Geophys. Res.*, **102**, 24545-24559.

PATACCA, E., P. SCANDONE, M. BELLATALLA, N. PERILLI and U. SANTINI (1988): L'Appennino meridionale: modello strutturale e palinspastica dei domini esterni, *Paper presented at the 74th Congress of the Società Geologica Italiana, Sorrento, Italy*, 67-69.

PATELLA, D. (1997): Introduction to ground surface self-potential tomography, *Geophys. Prospect.*, **45**, 653-681.

PATELLA, D., A. TRAMACERE and R. DI MAIO (1997): Modelling earth current precursors in earthquake prediction, *Ann. Geofis.*, **40** (2), 495-517.

PESCATORE, T., P. RENDA and M. TRAMUTOLI (1988): Rapporti tra le unità lagonegresi e le unità sicilidi nella media valle del Basento (Appennino Lucano), *Mem. Soc. Geol. Ital.*, **41**, 353-361.

REVIL, A. and P.A. PEZARD (1998): Streaming electrical potential anomaly along faults in geothermal areas, *Geophys. Res. Lett.*, **25**, 3197-3200.

SCHOLTZ, C.H. (1990): *The Mechanics of Earthquakes and Faulting* (Cambridge University Press), pp. 439.

TERTULLIANI, A., M. ANZIDEI, A. MARAMAI, M. MURRU and F. RIGUZZI (1992): Macroseismic study of the Potenza (Southern Italy) earthquake of 5 May 1990, *Natural Hazards*, **6**, 25-38.

VAROTSOS, P., K. ALEXOPOULOS and M. LAZARIDOU (1993): Latest aspects of earthquake prediction in Greece based on seismic electric signals, *Tectonophysics*, **224**, 1-39.

ZLOTNICKI, J., M. FEUILLARD and G. HAMMOUYA (1994): Water circulations on La Sufrière volcano inferred by self-potential surveys (Guadeloupe, Lesse Antilles). Renew of Volcanic Activity?, *J. Geomagn. Geoelectr.*, **46**, 797-813.